

# < EQUALITY >

Efficient QUantum ALgorithms for IndusTrY

WP3 Stack Integration

## D3.1 Specifications on quantum hardware and low-level implementations

Version: 4.0

Submission date: 25/10/2023

**AIRBUS**

Capgemini

 DA VINCI LABS

 **Fraunhofer**  
ENAS

 **DLR**  
Deutsches Zentrum  
für Luft- und Raumfahrt  
German Aerospace Center

*Inria*

 **Universiteit**  
**Leiden**  
The Netherlands

 **PASQAL**

## 1. Document control

<b>Project title</b>	Efficient QUantum ALgorithms for IndusTrY
<b>Project acronym</b>	EQUALITY
<b>Call identifier</b>	HORIZON-CL4-2021-DIGITAL-EMERGING-02
<b>Grant agreement</b>	101080142
<b>Starting date</b>	01/11/2022
<b>Duration</b>	36 months
<b>Project URL</b>	<a href="http://equality-quantum.eu">http://equality-quantum.eu</a>
<b>Work Package</b>	WP3 Stack Integration
<b>Deliverable</b>	D3.1 Specifications on quantum hardware and low-level implementations
<b>Contractual Delivery Date</b>	M12
<b>Actual Delivery Date</b>	M12
<b>Nature<sup>1</sup></b>	R
<b>Dissemination level<sup>2</sup></b>	PU
<b>Lead Beneficiary</b>	PASQAL (Qu&Co AI BV)
<b>Editor(s)</b>	Panagiotis Barkoutsos, Lorenzo Cardarelli
<b>Contributor(s)</b>	Panagiotis Barkoutsos, Lorenzo Cardarelli
<b>Reviewer(s)</b>	Kirill Shiianov, Max Schammer, Pablo-David Rojas
<b>Document description</b>	This deliverable will demonstrate the implementation of the developed algorithm primitives on specific hardware types per the measurement of the exploitation strategies' performance. It will include the process documentation as well.

<sup>1</sup>R: Document, report (excluding the periodic and final reports); DEM: Demonstrator, pilot, prototype, plan designs; DEC: Websites, patents filing, press & media actions, videos, etc.; DATA: Data sets, microdata, etc.; DMP: Data management plan; ETHICS: Deliverables related to ethics issues.; SECURITY: Deliverables related to security issues; OTHER: Software, technical diagram, algorithms, models, etc.

<sup>2</sup>PU – Public, fully open, e.g., web (Deliverables flagged as public will be automatically published in CORDIS project's page); SEN – Sensitive, limited under the conditions of the Grant Agreement; Classified R-UE/EU-R – EU RESTRICTED under the Commission Decision No2015/444; Classified C-UE/EU-C – EU CONFIDENTIAL under the Commission Decision No2015/444; Classified S-UE/EU-S – EU SECRET under the Commission Decision No2015/444

## 2. Version control

Version	Editor(s) Contributor(s) Reviewer(s)	Date	Description
0.1	Lorenzo Cardarelli, Panagiotis Barkoutsos	2.10.2023	Creation of intermediate document structure and content
0.2	Lorenzo Cardarelli, Panagiotis Barkoutsos	3.10.2023	Scientific revision and input for intermediate document
0.3	Kirill Shiiarov	13.10.2023	Scientific revision of intermediate document
0.4	Lorenzo Cardarelli	15.10.2023	Scientific corrections and complementary information for intermediate document
0.5	Max Schammer	16.10.2023	Scientific and content revision of intermediate document
0.6	Lorenzo Cardarelli	18.10.2023	Scientific corrections and complementary information for intermediate document
0.7	Panagiotis Barkoutsos	19.10.2023	Scientific corrections and complementary information for intermediate document
0.8	Pablo-David Rojas	20.10.2023	Overall format of intermediate document
1	Kirill Shiiarov, Pranjal Dhole, Pablo-David Rojas	23.10.2023	Final scientific reviews to intermediate document
2	Lorenzo Cardarelli, Panagiotis Barkoutsos	23.10.2023	Document finished by editors and contributors
3	Kirill Shiiarov, Pranjal Dhole, Pablo-David Rojas	24.10.2023	Final formatting to intermediate document
4	Pablo-David Rojas	25.10.2023	Document released by Technical Project Lead

### 3. Abstract

A quantum revolution is unfolding, and European scientists are on the lead. Now, it is time to take decisive action and transform our scientific potential into a competitive advantage. Achieving this goal will be critical to ensuring Europe's technological sovereignty in the coming decades.

EQUALITY brings together scientists, innovators, and prominent industrial players with the mission of developing cutting-edge quantum algorithms to solve strategic industrial problems. The consortium will develop a set of algorithmic primitives which could be used as modules for various industry-specific workflows. These primitives include differential equation solvers, material simulation algorithms, quantum optimisers, etc.

To focus our efforts, we target eight paradigmatic industrial problems. These problems are likely to yield early quantum advantage and pertain to the aerospace and energy storage industries. They include airfoil aerodynamics, battery and fuel cell design, space mission optimisation, etc. Our goal is to develop quantum algorithms for real industrial problems using real quantum hardware. This requires grappling with the limitations of present-day quantum hardware. Thus, we will devote a large portion of our efforts to developing strategies for optimal hardware exploitation. These low-level implementations will account for the effects of noise and topology and will optimise algorithms to run on limited hardware.

EQUALITY will build synergies with Quantum Flagship projects and Europe's thriving ecosystem of quantum start-ups. Use cases will be tested on quantum hardware from three of Europe's leading vendors and two HPC centres. The applications targeted have the potential of creating billions of euros for end-users and technology providers over the coming decades. With EQUALITY, we aim at playing a role in unlocking this value and placing Europe at the centre of this development. The project gathers 9 partners and has a budget of €6M over 3 years.

### 4. Consortium

The EQUALITY consortium members are listed below.

Legal Name on Grant Agreement	Short name	Country
CAPGEMINI DEUTSCHLAND GMBH	CAP	DE
QU & CO AI BV	QC	FR
AIRBUS OPERATIONS GMBH	AOG	DE
DEUTSCHES ZENTRUM FUR LUFT - UND RAUMFAHRT EV (DLR)	DLR	DE
FRAUNHOFER GESELLSCHAFT ZUR FORDERUNG DER ANGEWANDTEN FORSCHUNG EV (FHG)	ENAS	DE
INSTITUT NATIONAL DE RECHERCHE EN INFORMATIQUE ET AUTOMATIQUE (INRIA)	INRIA	FR
UNIVERSITEIT LEIDEN (ULEI)	ULEI	NL
DA VINCI LABS	DVL	FR

## 5. Disclaimer

This document does not represent the opinion of the European Union or European Commission, and neither the European Union nor the granting authority can be held responsible for any use that might be made of its content.

This document may contain material which is the copyright of certain EQUALITY consortium parties and may not be reproduced or copied without permission. All EQUALITY consortium parties have agreed to the complete publication of this document. The commercial use of any information in this document may require a license from the proprietor.

Neither the EQUALITY consortium nor a certain party of the EQUALITY consortium warrants that the information contained in this document are capable of use nor that the use of the data is free from risk. It accepts no liability for loss or damage anyone suffers using this information.

## 6. Acknowledgement

This document is a deliverable of EQUALITY project. This project has received funding from the European Union's Horizon Europe research and innovation programme under grant agreement N° 101080142.

## 7. Table of Contents

Document control .....	2
Version control .....	3
Abstract .....	4
Consortium .....	4
Disclaimer .....	5
Acknowledgement .....	5
Table of Contents.....	6
List of Abbreviations .....	7
List of Figures.....	8
List of Tables .....	9
1. EXECUTIVE SUMMARY .....	10
2. HARDWARE PLATFORMS .....	11
NEUTRAL ATOM BASED QUANTUM HARDWARE.....	11
ION TRAP BASED QUANTUM HARDWARE .....	14
SUPERCONDUCTING QUBITS QUANTUM HARDWARE .....	15
3. ALGORITHMIC IMPLEMENTATION IN DIFFERENT HARDWARE ARCHITECTURES.....	18
VARIATIONAL QUANTUM EIGENSOLVER (VQE) .....	18
DIFFERENTIABLE QUANTUM CIRCUITS .....	23
4. COMPARISON BETWEEN THE DIFFERENT TARGETTED ARCHITECTURES .....	26
DEVICE SPECIFICATIONS.....	26
DEVICE SPECIFICATION ASSUMPTIONS .....	28
ALGORITHM SPECIFICATION ASSUMPTIONS .....	31
RESULTS .....	32
5. CONCLUSIONS .....	36
6. BIBLIOGRAPHY.....	37

## 8. List of Abbreviations

WP	Work package
DQC	Differentiable Quantum Circuits
VA(s)	Variational Algorithm(s)
QEK	Quantum Evolution Kernel
QC(s)	Quantum Computer(s)
AOM	Acousto-Optic laser Modulator
EOM	Electro-Optic laser Modulator
CZ	Controlled Z
AMO	Atomic, Molecular, and Optical
MS	Mølmer and Sørensen
QCCD	Quantum Charge Coupled Device
UCC	Unitary Coupled Cluster
PINN(s)	Physics Informed Neural Network(s)
UFA	Universal Function Approximator
QAOA	Quantum Approximate Optimization Algorithm
NA	Neutral Atom
IT	Ion Trap
SC	Super Conducting

## 9. List of Figures

Figure 1: A schematic of the Variational Quantum Eigensolver.....	19
Figure 2: VQE of the H <sub>2</sub> molecule with trapped ions. (Left panel) - quantum circuits implementing the Unitary Coupled Cluster Singles and Doubles (UCCSD) operator expressed in terms of a spin-Hamiltonian after BW or JW mapping. The UCCSD encoding is based on well-known classical quantum chemistry techniques. (Right panel) Energy landscape of hydrogen's ground state. The reference line indicates theoretical predictions, while other curves represent variations in qubit count, input states, encoding methods, and gate fidelity .....	21
Figure 3: Schematics of the PINN (top) and DQC (bottom) algorithms. The two differ in the nature of the UFA (classical neural network vs quantum circuit) and in the backpropagation methodology (automatic differentiation vs e.g., parameter shift rule), but present overall analogous workflow. ....	24
Figure 4: Schematic representation of the QEK algorithm. An input graph is encoded into a Hamiltonian H <sub>G</sub> , which is used in a parametrized sequence, alternating evolution with H <sub>G</sub> and pulses with Hamiltonian H <sub>i</sub> . An observable is measured at the end of the pulse, yielding a bitstring. From this bitstring, a probability distribution is extracted, out of which the graph kernel is computed, as a distance on probability distributions. The precise form of the pulse sequence is determined through training on a graph data set.....	25
Figure 5: Execution times for the different hardware platforms and algorithms under consideration. Different colors denote different algorithms and different bar fillings denote current (solid bars) and future (striped bars) architectures. For each algorithm we record the execution time for Neutral Atom (NA), Superconducting (SC) and Ion Trap (IT) based devices. ....	32
Figure 6: Ratio between the single circuit execution (shot) over the available decoherence time of the specific qubit architecture. Different colors denote different algorithms and different bar fillings denote current (solid bars) and future (striped bars) architectures. For each algorithm we record the relevant ratio for Neutral Atom (NA), Superconducting (SC) and Ion Trap (IT) based devices. ....	33
Figure 7: Feasibility of Algorithms in Superconducting-qubit-based platforms in dependence of 2-qubit gate fidelity and coherence time .....	35
Figure 8: Feasibility of Algorithms in Ion-Trap-qubit-based platforms in dependence of 2-qubit gate fidelities and gate time.....	35



## 10. List of Tables

Table 1: Specification of Different Hardware Platforms (QPU and Algorithmic parameters) under consideration .....	27
Table 2: Comparison of execution times for all three algorithms and all three hardware platforms, experiment (as <i>current</i> ) and prediction (as <i>future</i> ) .....	34

## 11. EXECUTIVE SUMMARY

This document is a deliverable of the EQUALITY project, funded under grant agreement number 101080142.

This deliverable is part of WP3 “Stack Integration” and is the backbone for ensuring the completion of Milestone 2:” Primitives will be tested on small-scale paradigmatic problems using noiseless emulators, e.g., small molecules, 1D differential equations, etc. Flaws on the algorithms will be identified and corrected before moving on to the next stage.” for our project. The main goal of this activity is to test our algorithmic developments on paradigmatic models and ensure that our code basis can now be integrated with different quantum computing architectures.

To ensure the success of our project, this deliverable is aimed at giving a comprehensive overview of three hardware technologies, that are considered to have the highest potential to bring practical quantum advantage sooner than the others, as well as three algorithms that may help obtaining this advantage. The choice of technologies to compare was made based on the following factors: scientific and technological maturity of the hardware, its wide adoption as a subject of R&D both in academia and industry, wide scope of research institutions exploring different implementations of technology, rich knowledge base of hardware-specific algorithmic implementations, and finally – particular suitability for near-term practical quantum advantage due to certain strong points in hardware specification (like fidelity, connectivity or scale).

The first part of the deliverable describes the three hardware technologies in detail, focusing on the principles of their operation, main strengths and weaknesses of each technology. It also aims to give some degree of perspective on the development of each technology based on the publicly available data.

The second part of this work focuses on three principal algorithms, developed within the Equality project: Differential Quantum Circuits (DQC), Variational Algorithms (VAs) and Quantum Evolution Kernel (QEK). Functioning of these algorithms is explained in technical details. Implementation aspects of each of these algorithms for each of the hardware is explored in detail. This part also concludes on the suitability of each hardware for each of the algorithms and outlines the perspective changes of this disposition.

The third part of this work is dedicated to a multifaceted comparison of the three hardware technologies in scope of their use for running the three key algorithms described previously in this work. It focuses on those aspects of both hard- and soft-ware technologies, that matter for the capability of their synergy to deliver value in real use cases in the short- and near-term perspective. This section also provides the results of experiments, conducted by the authors to identify the real-world performance of each of these technology stacks. Important result of the research presented in this section is the proof of mutual suitability of certain hardware technologies with certain algorithmic realisations. This confirms the correctness of technological scoping of the Equality project. Successful testing of the algorithms on various hardware concludes reaching the Milestone 2 of the project and ensures the momentum of its advancements.

Altogether, this work concludes on the correctness of the approach taken by the Equality project: to develop the core algorithms at the same time the hardware technologies mature, to

be ready to deliver the practical value the soonest possible. It also serves a key to identify the most suitable pairs of hardware-software, which further facilitates the value delivery for the relevant industry use-cases.

Key words: *quantum algorithms, quantum software stack, qubit technologies, algorithms and hardware co-design*

## 12. HARDWARE PLATFORMS

Quantum computing is today a focal point of frontier research and innovation. The main stimulus behind the exploration of quantum computers arises from their potential to outperform classical counterparts in resolving problems in certain domains, either by achieving superior performance, higher speed, or tackling challenges that classical computing methods inherently cannot resolve.

The design, development and construction of a useful quantum computing unit is a worldwide ongoing effort, that involves a wide range of expertise and skills: cryogenics, quantum hardware engineering, theory of quantum algorithms and error correction, software development, funding and policy expertise. Different approaches to realize the computer exist, each leveraging on distinct physical systems for the generation, linkage, and control of qubits. In this Section, we will specifically review three different hardware platforms, based on neutral atoms, trapped ions, and superconductors. These constitute also the basis of our discussion on hardware implementation of quantum algorithms, presented in Section 3.

### NEUTRAL ATOM BASED QUANTUM HARDWARE

Arrays of neutral atoms manipulated by light beams are a solid and scalable technology to build useful quantum computers [Saffman2010]. Several elements contribute to its success. Hinging on the Nobel-prize winning technology of optical tweezers for trapping and displacing particles [Ashkin2018], this approach offers the unique possibility to spatially arrange the qubits in custom one, two and three-dimensional arrays. Moreover, the intrinsic scalability of the arrays, related to the number of atoms that a system of lasers can trap in a certain spatial region, opens prospects of increasing the number of qubits to the range of 100-1000 qubits [Henriet2020]. In this architecture, the qubit state is embedded in long-living electronic states, which guarantees a large ratio between the qubit coherence time and the cumulative gate operations time [Shi2022, Henriet2020].

A distinctive aspect of the neutral atom architecture lies in its compatibility with a hybrid analog and digital approach. As demonstrated in Ref. [Dodd2002], universal quantum computation can be performed using local unitary operations and any entangling interaction. This means that a generic unitary can be constructed using sequences of, e.g., Ising-type coupling which is native in Rydberg atoms arrays. In fact, numerical analyses [ParraRodriguez2020] showed the advantage of an analog-digital protocol over a pure digital approach in constructing relevant XZ-type Hamiltonians; the advantage is realized in higher fidelity and lower computational time, both in ideal and realistic scenarios. In the NISQ era, characterized by the constraint of small, error-prone quantum computing prototypes and limited evidence of significant business advantages, an analog quantum computing approach appears therefore better poised to provide immediate value. As the technological progress reaches maturity, a natural transition to a high-performance digital mode is foreseeable to occur.

## Architecture

Let us gain a primary understanding of the techniques and particulars of this approach to quantum simulation and computing. The main constituents of a platform confining and controlling cold neutral atoms in optical lattices are here summarized. Building upon decades of academic experience and development, the trapping routine is a well tried-and-tested one [Browaeys2020, Schreck2021]. As a starting point, a dilute atomic vapor at room temperature is formed in an ultra-high vacuum chamber. A first cooling operation brings the sample close to the Doppler temperature, typically by means of a Zeeman slower. The ensemble is confined by a first set of lasers in a  $1\text{mm}^3$  region, by what is called a 3D magneto-optical trap. Then, another laser system isolates individual atoms within this ensemble. This technique is based on the laser's electromagnetic field exerting a force on the particles that pushes them towards regions of higher beam intensity, effectively trapping them at the beam's focal point. Using lenses, the trapping beam is focused down to multiple regularly arranged spots of about  $1\ \mu\text{m}$  diameter. These needles of light are called optical tweezers. Within a trapping volume of a few  $\mu\text{m}^3$ , each tweezer can host at most one single atom at a time. The number of tweezers and their arrangement in arbitrary 1D, 2D or 3D geometries are fully tailored by holographic methods [Nogrette2014]. Spatial light and phase modulators placed before the lens provides control on the phase and intensity pattern of the tweezers. In light of their grade of pliability, neutral atom platforms present a unique potential of scalability of the atomic grid, hence of the number of qubits.

Lasers serve as a pivotal component for neutral atom quantum processing units. The operations predominantly utilize semiconductor lasers, commonly known as laser diodes. For high-power applications, fibre lasers are becoming the preferred choice due to their compact size, efficiency, enhanced beam quality, and superior thermal management [Zervas2014]. With the aim to broaden the traps for scaling up the qubit count, there is a growing requirement for more powerful lasers. This demand is propelling the relevance and exploration of fibre lasers, positioning them as a promising frontier for applications in neutral atom trapping. Currently limited by the performance and power of the optical system generating the optical tweezers, the size of a quantum register in neutral atoms is thus fated to grow as new generations of lasers are developed and released.

Unlike trapped ions, neutral atoms do not naturally interact but below very short distances. To generate entanglement between the qubits, it is necessary to engineer a long-distance coupling. A long-range interaction can be activated by exciting, on both atoms, the valence electron to a state with very large principle number, known as Rydberg state. Interactions between dipolar atoms are typically modelled as either dipole-dipole or van der Waals, depending on the Rydberg states configuration. Dipole-dipole interactions arise from the resonant exchange of virtual photons between atoms and result in an inter-atomic potential scaling with the inter-nuclei distance as  $1/r^3$ . The Van der Waals potential is proportional to  $1/r^6$  and arises from non-resonant exchange of virtual photons, a second-order process in perturbation theory [Adams2020]. Either kind extends for a range of the order of microns, which is a distance on the same scale as that of the tweezers grid. The dipole-mediated interaction is the essential element enabling the design of entangling operations for quantum computation purposes on neutral atom platforms. Thanks to their long-range coupling, neutral atoms can therefore uniquely support the generation of entanglement between any individually addressable pair or group of atoms within a large spatial region, enabling effective all-to-all interactions.

## Qubit encoding

Let us now come to the encoding and manipulation of quantum information in this architecture. With single trapped atoms as a support, one can encode a qubit algebra on a pair of electronic states. Which pair to choose depends on the atomic species utilised, on the computational approach considered (digital vs analog), and on other factors.

Digital computing requires qubits with major decoupling from the environment to prevent corruption of the logical state during the algorithm execution, e.g., due to decoherence. In this case, a couple of hyperfine states suit the cause since they have low radiative coupling to the electromagnetic environment and enjoy a very long lifetime as compared to the time scale of the computation [Kleine2011, Wurtz2023]. Single-qubit rotations are realized by stimulating with a laser the transition of the valence electron between these two energy levels. The atom-laser interaction is characterized by the Rabi frequency (proportional to the amplitude of the laser field), the detuning (the difference between the two-level resonance and the field frequencies) and their relative phase. The control over these elements, achieved via acousto- and electro-optic laser modulators (AOM and EOM), allows to realize arbitrary Bloch sphere rotations on a physical system [Henriet2020].

## Gate-based quantum information processing

In quantum information theory, it is common knowledge that universal quantum computation can be attained with no more than single rotations and a two-qubit controlled gate. Different schemes exist to realize a two-atoms Controlled-Z (CZ) gate [Jaksch2000] using dipolar Rydberg interaction [Isenhowe2010, Levine2019]. One protocol dictates the application of pi-pulses, resonant with the  $|0\rangle$ -to-Rydberg transition, sequentially on the control and target atoms. The detuning arising by either the energy gap with the  $|1\rangle$ -to-Rydberg transition or by the Rydberg blockade makes such that a  $-1$  phase is picked by all two-atom states except for the  $|11\rangle$ , thus creating the logic of the CZ gate. The gate can be performed within  $\mu\text{s}$  with a measured fidelity of 94.1% [Levine2018]. Present experiments, bounded by their current technical limitations, allow to stack more than a hundred repetitions of this gate before decoherence overshadows the process.

## Analog-digital quantum information processing

The analog-digital approach introduced above considers different states configurations [Michel2023]. One option is that  $|0\rangle$  be an electronic ground state and  $|1\rangle$  a Rydberg state. Then, the atoms experience a Van der Waals interaction corresponding to a density-density, or "ZZ", Ising Hamiltonian:

$$H_I = \sum_{i>j} \frac{C_6}{r_{ij}^6} n_i n_j$$

If, instead, one chooses two dipole-coupled Rydberg states (e.g.,  $|0\rangle = |nS\rangle$  and  $|1\rangle = |nP\rangle$  for large  $n$ ), the interaction is resonant and realizes a so-called XY or *flip-flop* term:

$$H_{XY} = \sum_{i \neq j} \frac{C_3}{r_{ij}^3} X_i X_j + \sum_{i \neq j} \frac{C_3}{r_{ij}^3} Y_i Y_j$$

These are two distinct examples of entangling operations that, as mentioned, suffice as such to attain universal quantum computation – see Ref. [Dodd2002]. Unlike digital quantum computation, where each pulse is strictly tasked with achieving a particular gate function and any deviation is considered an error, analog pulses offer flexibility. This flexibility is advantageous as it allows for the exploration of potentially more diverse entangling patterns. Furthermore, given that any entangling operation can achieve universal quantum computation, rather than straining to improve the pulses realizing a certain logical gate, in the analog framework one can opt for selecting the pulse that is optimal under the given experimental conditions, considering factors like stability, reproducibility, and precision. The primary significance of such a pulse is not necessarily in replicating a specific gate such as CNOT, but rather in its inherent ability to facilitate quantum entanglement. This ability might exceed the effectiveness of certain designated gate sequences.

## Perspectives

To sum up, Rydberg atoms offer a promising avenue for quantum processor development, despite being newer compared to other approaches in the domain. This design employs laser cooling and trapping methods to manipulate the placement of neutral atoms via optical or microwave pulses and the manipulation of the quantum states. Advantages of this method include extended coherence durations, scalability in both 2D and 3D, and good connectivity due to long-range Rydberg interactions.

## ION TRAP BASED QUANTUM HARDWARE

Ion trapping stands as a well-established and thoroughly investigated field within the domain of Atomic, Molecular, and Optical (AMO) physics, enjoying both long-standing history and widespread adoption [IonTrappingWW]. Thanks to its enduring presence and suitability for fundamental algorithmic operations, the trapped-ion architecture plays a prominent role on the stage of quantum processors.

### Architecture

This approach uses electric and magnetic fields to trap ions in a vacuum chamber and manipulate their quantum states by optical or electrical means. The particulars of a trapped-ion experiment can vary significantly, primarily depending on the specific atomic species of the particles manipulated. Usually a trade-off between experimental hurdles, expertise in the team and ultimate advantages in the quantum computation determines the choice of the atomic species. At this stage, the  $^{40}\text{Ca}^+$  isotope of Calcium ranks among the most adopted species, along with isotopes of other alkaline-earth metals as Barium, Beryllium and Strontium. Another broadly used species is Ytterbium, a lanthanide element [IonTrappingWW].

In trapped-ion experiences, an experimental cycle begins with the sublimation of a thermal solid source, e.g., Calcium. The vapour beam is photoionized via a two-photon transition and then confined in a Paul trap [FSKYT]. Cooling techniques reduce the temperature of the hot cloud from 100-1000 Kelvin to sub-Doppler regimes where the atoms arrange themselves in a spatially regular geometry known as Coulomb crystal. Finally, optical pumping and sideband cooling further reduce the entropy and bring the system onto its electronic ground-state.

## Qubit encoding

The encoding of a qubit on an ion requires two electronic levels, that be accessible by the valence electron, in a controlled fashion. In this regard, multiple options are available to control qubits, from optical qubits (visible spectrum, infrared) to Zeeman and hyperfine qubits (microwaves). An optimal choice weighs in technical or performance considerations.

## Gate-based quantum information processing

Trapped-ion architectures can lay claim to remarkable control on single qubit rotations and two-qubit entangling operations, and a high fidelity of both of these gates [Bruzewicz2019]. In the case of optical states, single-qubit gates have achieved fidelities up to 99.995% with a gate time of 5  $\mu\text{s}$  [Bermudez2017], while microwave gates strike single-ion fidelities of 99.9999% in 12  $\mu\text{s}$  [Harty2014]; both experiments used  $\text{Ca}^+$  and showed low crosstalk. Entangling gates can be realized through different protocols leveraging on the shared motional modes to generate coupling between ions. The first proposal of a two-ions gate was made by Cirac and Zoller [Cirac1995] and requires the ions to be in the motional ground state. This requirement is dropped in the method proposed by Mølmer and Sørensen (MS) [Sørensen1999]. The MS gate is presently a standard way to implement the CNOT gate and scores a fidelity of 99.8% in a 27.4  $\mu\text{s}$  cycle period [Ballance2015]. Other forms of geometric phase gates allow too to hit 99.8% fidelity in hyperfine qubits in 1.6  $\mu\text{s}$  [Schäfer2018].

The coherence time of trapped ion qubit states can extend up to 50s on hyperfine states of an individual  $^{43}\text{Ca}^+$  atom [Harty2014] and up to 2s on Zeeman states of an individual  $^{40}\text{Ca}^+$  atom [Ruster2016]. Hence, trapped ions shine for an incredible ratio between the qubit coherence time and the time scale of gate operations, an aspect that makes this technology strong and promising, particularly with regard to hardware realizations of deep circuit quantum algorithms.

## Perspectives

The ion-based approach has been successfully used to manufacture quantum computers with high levels of coherence and very high connectivity. Calculation speed and scaling to large numbers of qubits remain a challenge, but recent advancements by companies like Quantinuum have set new records in quantum volume, showcasing a balanced improvement across crucial parameters such as qubit connectivity and gate fidelity [QuantinuumVolume]. The advent of architectures like the Quantum Charge Coupled Device (QCCD) heralds a promising pathway towards effective qubit manipulation and system scalability [QuantinuumQCCD]. International collaborations and investments, such as the German Quantum Computing Initiative, reflect a growing global recognition and support for the trapped-ion quantum computing platforms [UnivQuantum]. Collectively, these developments signify a vibrant trajectory for trapped-ion quantum computing, progressively edging closer to addressing the pivotal challenges of calculation speed and scalability, vital for real-world quantum computing deployment.

## SUPERCONDUCTING QUBITS QUANTUM HARDWARE

This approach uses superconducting resonant circuits to build qubits. The circuits operate at very low temperatures, allow for fast gate operations, but currently still suffer from low coherence times and limited connectivity.

## Architecture specifications

Superconductivity is a quantum mechanical phenomenon observed in certain materials, like Niobium or Aluminum, at very low temperatures. In a superconducting state, these materials have zero electrical resistance and can conduct electric current without any energy loss. Electrons within a material in superconductive state exhibit collective behaviour, being described by a common wavefunction, forming a natural quantum system, which can be controlled externally via magnetic fields and microwave pulses. The heart of a superconducting qubit is the Josephson junction, which is a nanoscale device made of two superconducting materials separated by a thin insulating barrier. The Josephson junction acts as an inductor and presents a discrete non-linear spectrum. The non-linearity ensures that any pair of states is separated by a unique energy gap, making the pair distinguishable and unambiguously addressable. The  $|0\rangle$  and  $|1\rangle$  states can thus be uniquely assigned to two levels of the energy spectrum. To perform quantum operations on a superconducting qubit, external microwave pulses or currents are applied to the Josephson junction. Altogether, microwave pulses, bias currents and magnetic fields allow for full control over the qubit energy spectrum, enabling quantum gates and operations to control qubit state. State measurements occur via coupling to a microwave resonator. By probing the resonator with microwaves and measuring the reflected signal, the qubit state can be determined. Like all qubit technologies, superconducting qubits are susceptible to decoherence, which is the loss of quantum information due to coupling with the environment. Researchers use various techniques, such as error correction codes and improved qubit designs, to mitigate decoherence effects and improve the qubits' quantum coherence time. Differently from most other technologies, instead, superconducting qubits benefit from the mature infrastructure developed for conventional semiconductor fabrication. This means that techniques for making precise, nanoscale structures are already well-established. As a result, the potential to manufacture many superconducting qubits on a single chip using standard lithographic techniques is already available, whereas to trap a large number of ions or neutral atoms requires technological advancements and the development of ad-hoc solutions.

## Qubit encoding

Like other types of qubits, superconducting qubits also represent quantum information as a two-level quantum system. The two primary states are often referred to as  $|0\rangle$  (ground state) and  $|1\rangle$  (excited state), analogous to classical binary 0 and 1. Advances in superconducting qubit technology are continually pushing the boundaries of quantum computing capabilities.

## Gate-based quantum information processing

A gate operation is achieved by sending microwave pulses. Josephson junctions, a type of superconducting tunnel junction, are critical components in superconducting qubits, enabling the non-linear behaviour required for these operations. The precise control and interaction of these pulses with superconducting qubits is crucial for the coherent manipulation and readout of quantum information, which in turn is foundational for advancing quantum computing technologies.

## Perspectives

Superconducting qubits are a versatile and promising platform for building quantum computers and quantum processors. They are used by various companies and research institutions to



explore and develop quantum algorithms and applications. In conclusion, superconducting qubits continue to be a pivotal player in the advancement of quantum computing, offering a pathway towards hardware scaling. While scaling up the hardware doesn't directly enhance coherence, having a large register allows to implement quantum error correcting codes - notably greedy in the number of ancilla qubits - which in turn helps in progressing towards fault-tolerant computation. Recent work from MIT has showcased a novel superconducting qubit architecture utilizing fluxonium qubits, which demonstrated remarkable accuracy in quantum operations, pushing the boundaries of error correction closer to practical realization [Ding2023]. Moreover, the collaborative endeavours with public research funders fuel and consolidate the efforts of quantum companies. A prime example of this is the partnership between VTT Technical Research Centre of Finland and IQM Quantum Computers, which aims to escalate their superconducting platform to a 50-qubit quantum computer by 2024. This ambitious venture, further backed by a substantial government budget, envisions scaling up to a 300-qubit quantum computer, thereby manifesting a solid commitment towards achieving quantum advantage [IQMVTT].

As the collaborative synergy among academia, industry, and government accelerates, the horizon for quantum computing, underpinned by superconducting qubits, continues to expand. These collective endeavours not only highlight the ongoing efforts to scale quantum computing but also underscore the potential for quantum solutions to tackle complex challenges across various domains, marking a substantial stride towards a new era of computational capability.

## 13. ALGORITHMIC IMPLEMENTATION IN DIFFERENT HARDWARE ARCHITECTURES

In this chapter we focus on the implementation aspect of the algorithms in low-level architectures and discuss the limitations of the different hardware architectures discussed in Chapter 2. We estimate the near-term feasibility and provide insights on possible limitations that we will encounter in implementing our algorithms in any of the architectures.

### VARIATIONAL QUANTUM EIGENSOLVER (VQE)

The Variational Quantum Eigensolver (VQE) is a quantum algorithm designed to find an approximation of the ground-state and of the energy of a given quantum system [Peruzzo2014, McClean2016]. VQE is a pivotal quantum algorithm, finding application in complex problems in quantum chemistry, materials science, and optimization. The algorithm employs parameterized quantum circuits to encode trial wavefunctions and optimizes the set of real-valued parameters to minimize the expected energy of the target quantum system.

To gain a deeper comprehension of this method, let us see it in action on a particularly compelling application in theoretical chemistry, such as the computation of the lowest energy eigenvector of a Hamiltonian modelling a molecular electronic structure. Finding this ground-state grants access to the physical properties of the system, whence the relevance of obtaining this solution. In this context, the Hamiltonian is primarily written in the first-quantization formalism, accounting for the kinetic energy and mutual interactions of all charged particles involved, nuclei and electrons. Quantum algorithms can treat the problem in this formulation already. Alternatively, one can consider the second-quantized representation of the Hamiltonian. The mapping occurs by picking a basis set, often molecular orbitals built as linear combination of Hydrogen-like atomic orbitals. A simple example often used to explain how VQE works for quantum chemistry simulations considers the  $H_2$  molecule. The second-quantized Hamiltonian is defined in terms of fermionic creation and annihilation operators acting on the chosen basis set, as the  $H_2$  molecular orbitals or some modification thereof. Since most quantum simulators work in a spin-like language, meaning operating Pauli rather than fermionic operators, one last mapping is due to represent the system model as a spin-Hamiltonian. This can be done using well-known canonical transformations. Lastly, in this picture, the qubits represent the orbitals and their occupation.

### VQE protocol

The basic elements and protocol of VQE are here described.

- **System Hamiltonian:** To begin with, it is necessary to represent the Hamiltonian of the physical system (the molecule) investigated in the form of an observable operator in a  $2^n$ -dimensional Hilbert space,  $n$  being the number of qubits in the QPU register.
- **Parametrized Ansatz:** VQE starts with the selection of a parameterized quantum circuit, also known as the circuit Ansatz. This quantum circuit is applied to a fixed initial quantum state and **outputs a trial wavefunction, which is the approximation of the sought-after state**, usually being the ground state of the target quantum system in quantum chemistry problems. The ansatz consists of a sequence of single- and multi-qubit quantum gates, such as Pauli rotations and CNOT gates or global entangling

pulses. Part of or all these gates depend on **parameters**  $\theta$  such as, e.g., the duration of the pulse or the angle of the rotation axis, which get updated during the optimization process.

- **Cost Function:** The objective of VQE is to find the set of parameters  $\theta$  that minimizes the expectation value  $E(\theta)$  of the system's Hamiltonian operator  $H$ . This corresponds to the energy of the quantum system and acts as a cost function for a classical optimization routine over the parameter space.
- **Classical Optimization:** VQE employs classical optimization algorithms to iteratively adjust the parameters  $\theta$  within the ansatz, to approach the minimal value of the cost function. Commonly used optimization techniques include first- and second-order gradient-based methods like the Adam optimizer or Quantum Natural Gradient descent or gradient-free methods [Tilly2022].
- **Cost function and optimization:** Within the classical optimization loop, to estimate the expectation value  $E(\theta)$  of the cost function, the quantum circuit is executed and measured multiple times on a quantum processor. A classical optimization algorithm determines how the parameters are updated after each iteration to approach the minimum of the cost function. Convergence criteria, such as achieving a certain level of parameter stability, are used to determine when to stop the optimization process.

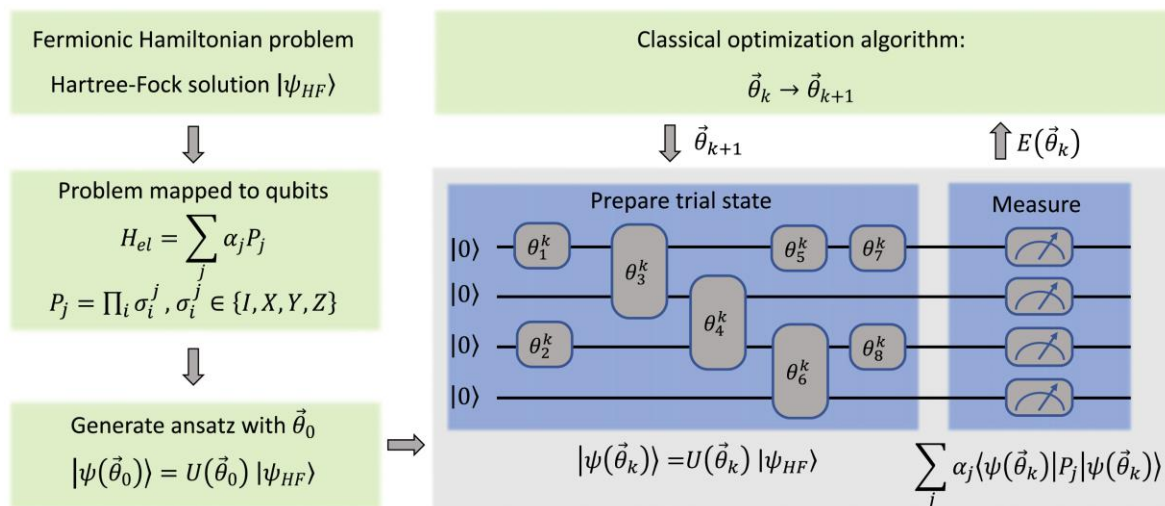


Figure 1: A schematic of the Variational Quantum Eigensolver.

Image from Fedorov et al. under CCA 4.0

An engaging series of VQE experiments on real quantum hardware spanned the last decade. In 2013, a first VQE demonstration was carried out on a photonic platform to investigate the  $\text{HeH}^+$  cation [Peruzzo2014]. In 2016, another significant experiment employed superconducting qubits [O'Malley2016] and reported on the first molecular calculation without the need for exponentially costly pre-compilation. A more advanced superconducting qubit implementation in terms of molecular size and resource scaling was published in Ref. [Kandala2017]. In that work, the authors conducted a theoretical analysis of the resource demands concerning circuit depth, revealing an advantageous scaling pattern for devices

featuring all-to-all qubit connectivity, an inherent property of both trapped-ion atoms and of neutral-atom with long-range interaction. Since then and continuing to the present day, a growing number of experiments have been conducted in this context, highlighting the ongoing pursuit of understanding and advancement in the field of variational quantum algorithms for molecular structure analysis.

### VQE application: hydrogen molecule ground-state

The execution of a VQE algorithm on a quantum processor normally requires adjustments to suit the platform particularities, regarding e.g., the available gate set and measurement operators or the state initialization. Let us review some experiences where the VQE algorithm has been executed on a selection of currently available QCs, including trapped ions [Hempel2018] and neutral atoms [Michel2023].

Congruously with the resources of the NISQ era devices, the target of the ground-state search in these studies are very simple molecules like  $H_2$ , Li-H or Be- $H_2$ . The second-quantized formulation of  $H_2$  reads as follows:

$$H_2 = \sum_{pq} h_{pq} a_p^\dagger a_q + \sum_{pqrs} h_{pqrs} a_p^\dagger a_q^\dagger a_r a_s$$

Common schemes to map this to a spin model are the Jordan-Wigner (JW) and the Bravyi-Kitaev (BK) transformations. The structure of the resource Hamiltonian, or the unitary operation applied to the initial state (Ansatz), can be chosen based on known properties of the target system. The structure of the Ansatz is of critical importance for the success of the algorithm and should somehow relate to the nature of the problem. It should be expressive enough to cover the areas of interest within the Hilbert space, yet - not too complex to be intractable for the classical optimization routine. For instance, [Hempel2018] uses the Unitary Coupled Cluster approach (UCC) to define a convenient parameterized operation, which, after a JW or BK mapping results in a simple circuit made of global entangling gates and a single-parameter Z rotation, as shown in Figure 2.

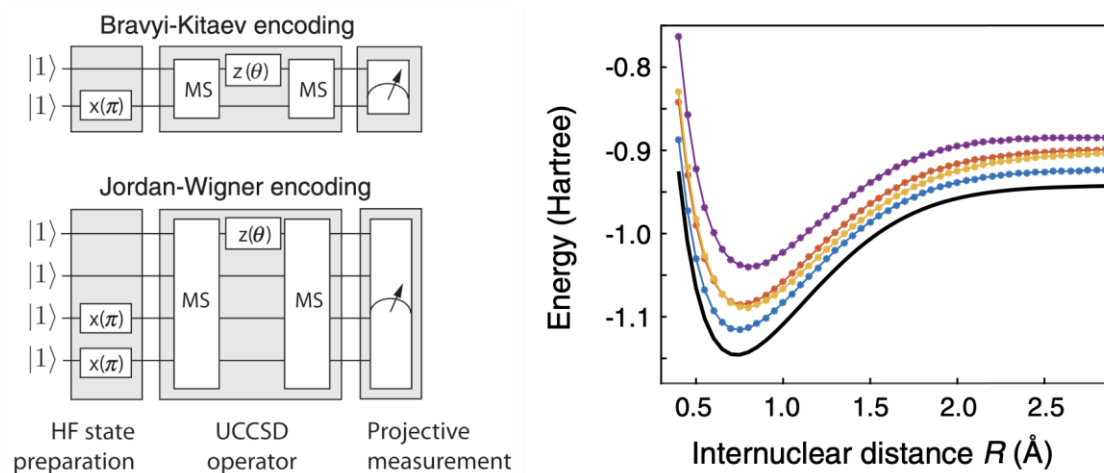


Figure 2: VQE of the  $H_2$  molecule with trapped ions. (Left panel) - quantum circuits implementing the Unitary Coupled Cluster Singles and Doubles (UCCSD) operator expressed in terms of a spin-Hamiltonian after BW or JW mapping. The UCCSD encoding is based on well-known classical quantum chemistry techniques. (Right panel) Energy landscape of hydrogen's ground state. The reference line indicates theoretical predictions, while other curves represent variations in qubit count, input states, encoding methods, and gate fidelity. Images from [Hempel et al.](#) under CCA 4.0

Under these circumstances, meaning with a single element  $\theta$  to optimize, it is possible to efficiently scan the whole parameter space to find the minimum to find the value of  $\theta$  corresponding to the minimum of the defined cost function, or infer it from a significant sample.

### VQE for H2 on quantum hardware: trapped ions

Various approaches have been explored for executing the VQE algorithm on trapped-ion-based quantum computing architectures. Early-days experiments [Shen2017] used internal energy levels of a single qubit as a basis for the Hamiltonian encoding. The method is hard to scale for larger molecules. Molecular alterations - such as structural deformations, changes in the vibrational frequency or in the normal modes - can be mapped to inherent operations in quantum optics by applying a harmonic approximation on the electronic potential energy surfaces. This approach allowed the authors of Ref. [Shen2018] to simulate on a chain of ions molecule's ionization processes due to photon absorption, as it occurs in the  $SO_2 \rightarrow SO_2^-$  process. By comparison, the second-quantized spin-Hamiltonian method described above results more general and in principle scalable to larger systems. In the experience reported there, Ref. [Hempel2018], the goal was the reconstruction of the ground state potential energy surface as a function of the inter-atomic distance  $R$ . As shown in the right panel of Figure 2, various configurations approximate with difference degree of accuracy the actual potential, with the configuration using the BK mapping and the state  $|01\rangle$  as an initial state leading to the best result. Reportedly, each VQE point took less than 1000 repetitions of the circuit.

### VQE for H2 on quantum hardware: neutral atoms

In addition to the cases presented above, an attempt to estimate the energy surface of H2 by running VQE on real quantum hardware was made also in neutral atoms set up [Michel2023]. There, the authors followed the same approach as above for the problem formulation and the Hamiltonian mapping. The entangling part of the resource Hamiltonian is the XY Hamiltonian

( $H_{XY}$  defined before), a fixed coherent exchange of neighboring spin states  $|10\rangle$  to  $|01\rangle$ . In addition, one can include time-dependent laser pulses, coupling the logical states. The pulses are characterized by a Rabi frequency  $\Omega(t)$  and a detuning  $\delta(t)$  of the field with respect to the resonant transition frequency, which translate into time-dependent X and Z Hamiltonian terms, with local or global addressability:

$$H_{drive} = \hbar \sum_{i=1}^N \left( \frac{1}{2} \Omega(t) X_i - \delta_i(t) n_i \right)$$

Numerical simulations showed that implementing this UCC ansatz on an analog-digital Quantum Processor would allow to hit below 5% error in about 4 hours operating at 3 Hz, using less than 36500 shots for each point.

Since this approach is hardly scalable to larger systems, novel customized approaches aiming at exploiting the capabilities of already available Rydberg QCs must be explored. Two alternatives to the resource Hamiltonian presented above were presented in Ref. [Michel2023]. The first one considers a sequence composed by alternating global pulses, corresponding to two non-commuting Hamiltonian. Another one introduces a time-dependent phase in the X term of  $H_{drive}$ . Besides pulse sequences in the processing stage, there is room for optimization also in the layout of the trapping array. One analogy behind the optimization of these coordinates would be, for instance, the resemblance between the interaction energy matrix and the target Hamiltonian. Comparative numerical analyses between these variants and the basic route presented above show moderate improvements [Michel2023]. These results should be viewed as a first benchmark of novel approaches and call for the development of further solutions able to leverage the unique potential of Rydberg quantum processors.

## VQE for H<sub>2</sub> on quantum hardware: superconducting qubits

Researchers used superconducting qubits to simulate the electronic structure and energy levels of H<sub>2</sub> to better understand its properties in multiple cases. The simulation of the H<sub>2</sub> was used as a benchmark problem for demonstrating hardware capabilities in the previous years. In Ref. [O'Malley 2016] researchers from Google reported the first electronic structure calculation performed on a quantum computer using a programmable array of superconducting qubits. The demonstration was based on the use of Quantum Phase Estimation and Variational Quantum Eigensolver algorithms, and the results were quite accurate with the basis set approximation that was used. For the case of the VQE algorithm, the use of UCC trial wavefunction was employed and the results gave clear indication for the potential of VQE in superconducting qubit platforms. Later, in Ref. [Kandala2017], the IBM researchers also demonstrated chemical simulations of H<sub>2</sub> (as well as other molecules) with superconducting qubits, using the so-called Hardware Efficient Trial wavefunctions. The main characteristic of these parameterized wavefunctions was that instead of using a structured/problem specific Ansatz the authors used all gates that were available in the superconducting qubit hardware to search the Fock space of the problem. This approach leverages all hardware capabilities available at that time to create a problem independent Ansatz that can be generalized for any other use case targeted with a Variational Algorithm. Following this work in Ref. [Kandala2018] the same team from IBM demonstrated the use of the superconducting qubit platforms within an error mitigated chemistry calculation with results approaching chemical accuracy for the simulated model. Numerous other publications and works from research groups can be found in the literature, but we focus on these seminal

works that were the first to simulate the  $H_2$  molecule on a superconducting qubit device and paved the road for electronic structure calculations with potential for scaling in state-of-the-art quantum computers.

## DIFFERENTIABLE QUANTUM CIRCUITS

Many relevant problems in industrial R&D, science, finance and beyond are modelled by differential equations.

Most of these equations can only be solved via numerical methods such as spectral or grid-based algorithms, which require significant computational effort. Furthermore, these approaches are inherently deterministic, and the solution can only be enhanced by increasing computational power, such as refining accuracy through further domain discretization. However, beyond these adjustments, the course of the algorithm and the outcome thereof are predetermined.

In recent years, a machine learning alternative has emerged, known as Physics Informed Neural Networks (PINN). The method considers a neural network  $N(x)$  that takes as input collocation points  $\{x\}$  from the domain of the target differential equation (DE), and trains it to approximate the unknown solution  $f(x)$  of the DE. Algorithmic differentiation allows to calculate exactly the derivatives of  $N(x)$  with respect to  $x$ ; these are used to build the cost function as a sum of the terms in the DE and update the network parameters.

DQC is a quantum algorithm inspired by PINNs. Similarly, to the classical machine learning approach, DQC proposes to train a parameterized framework to find a good approximator of the solution of a DE. This occurs by defining a quantum circuit  $U(x)$  with trainable parameters that can represent a function in the same domain and codomain of  $f(x)$  and that, after a loss-function driven optimization, would mimic well the solution of the DE. We hereafter refer to  $N(x)$  and  $U(x)$  as universal function approximators (UFAs).

The main elements of DQC are the quantum feature map and the differentiable variational circuit. Let us see these in detail.

- *Feature Map.* For the variational quantum circuit to act as an approximator of  $f(x)$ , the variable  $x$  must be encoded in the quantum circuit. The rule is to associate a value of  $x$  (collocation points) to a unique set of operators acting on the input state, for all the collocation points in the equation's domain: this is called *feature mapping* and is a more robust approach than the common encoding in the amplitude of the wave function.

There are different ways to realize a variable mapping. One such example is the product feature map [Kyriienko2021], in which one applies a layer of Pauli rotations whose phase is determined by a function  $\phi(x)$ . In this regard, a valid choice would be  $\phi(x) = \arcsin(x)$ . Equipping the function  $\phi(x)$  with a second dependency generally associated to the qubit index  $j$ , as  $\phi_j(x) = n_j \arcsin(x)$ , enriches considerably the map.

In fact, the gate  $\exp\left(-i \frac{2n_j \arccos(x)}{2} Y_j\right)$  can be decomposed onto a unitary operation with matrix elements defined by degree- $n$  Chebyshev polynomials of first and second kind, denoted as  $T_n(x)$  and  $U_n(x)$ , respectively.

Chebyshev polynomials form an optimal basis set to approximate any smooth function in the sense of the uniform  $L^\infty$  norm. Increasing the number of qubits in the register or adding layers with terms of different degree  $n$  to the feature map greatly enriches the basis set. In practical terms, as polynomials chain together and morph between two kinds and their degrees, the largely enriched basis set offers a more accurate fit.

- *Differentiable circuits.* The differentiability property of the gates in the feature map and in the circuit allows to calculate without numerical approximation the derivative of  $F(x)$ , analogously to algorithmic differentiation. This property is guaranteed by the adoption of a certain family of gates, such as the Pauli rotations, equipped with gate-analytical derivatives.

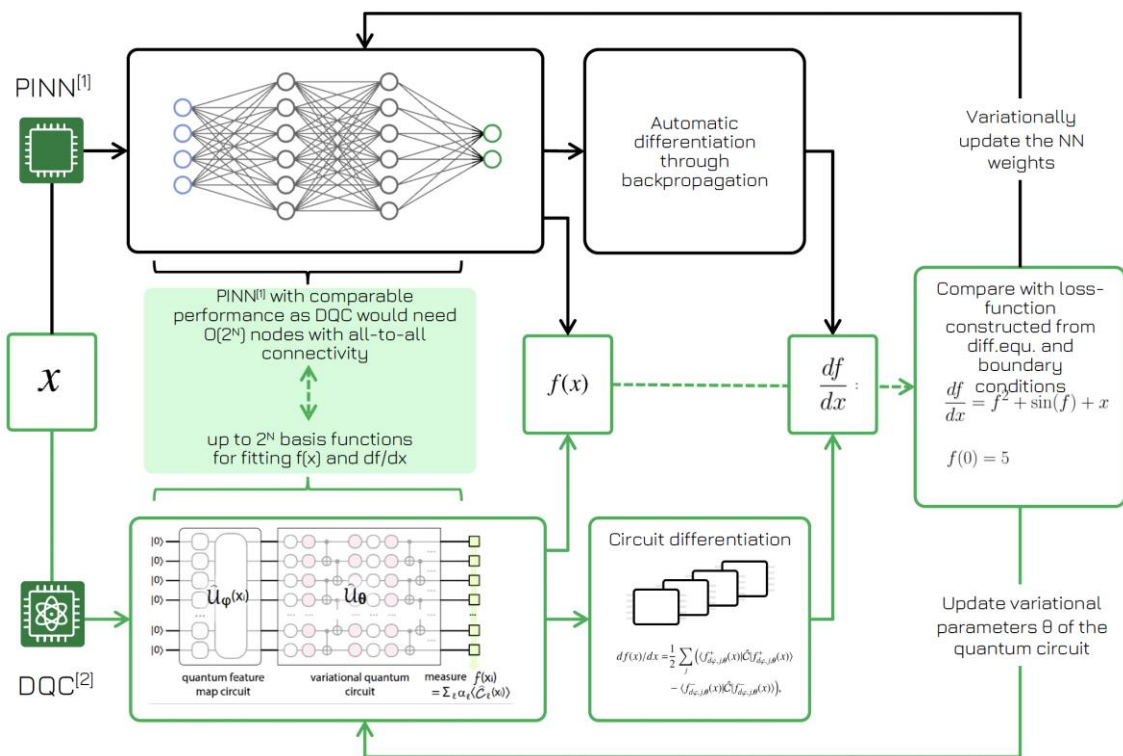


Figure 3: Schematics of the PINN (top) and DQC (bottom) algorithms. The two differ in the nature of the UFA (classical neural network vs quantum circuit) and in the backpropagation methodology (automatic differentiation vs e.g., parameter shift rule), but present overall analogous workflow.

## QUANTUM EVOLUTION KERNEL

Complex systems are encountered in various scientific and analytical disciplines. These systems are often characterized by a data-intensive nature and a connected structure, as it is the case for social networks, transportation systems, protein-protein interaction networks or sequence assembly. Understanding them requires the identification and analysis of prevalent patterns.

A convenient method to represent and study these systems is through graphs, a mathematical structure that captures entities as nodes and their relationships as edges. Graph representation is particularly advantageous because it offers a clear visualization of complex relationships, can efficiently handle vast datasets, and is supported by a rich suite of analytical



and numerical algorithms. Machine learning has extensively explored pattern recognition in graph-structured data, through methods called graph kernels. At their core, graph kernels work by associating each graph with a feature vector that captures its key characteristics, and then computing the similarity between these vectors, often as a scalar product. Despite interesting results attained in recent years, the algorithmic complexity and computational costs of graph-kernel methods pose challenges when dealing with large graphs.

Quantum computing holds promise in addressing classically intractable computational challenges. Quantum Evolution Kernel (QEK) is a versatile and easily scalable quantum algorithm introduced by PASQAL, potentially introducing advantage over classical kernel methods. The QEK algorithm unfolds as follows.

The information of a graph is encoded in the parameters of a tunable Hamiltonian. The topology of interactions of the Hamiltonian embeds that of the graph under study. Acting on an array of qubits, the Hamiltonian imprints the graph topology on the quantum state. After a sequence of parametrized pulses alternating with the Hamiltonian-driven evolution, a carefully chosen observable is measured to estimate the probability distribution of the graph.

This procedure is similar to the Quantum Approximate Optimization Algorithm (QAOA), or to the optimal control in a continuous parametrization of the Hamiltonian.

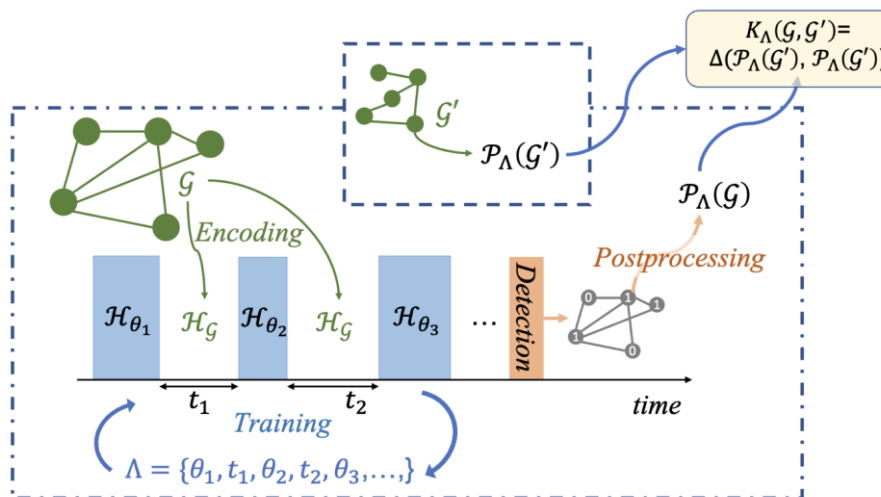


Figure 4: Schematic representation of the QEK algorithm. An input graph is encoded into a Hamiltonian  $H_G$ , which is used in a parametrized sequence, alternating evolution with  $H_G$  and pulses with Hamiltonian  $H_i$ . An observable is measured at the end of the pulse, yielding a bitstring. From this bitstring, a probability distribution is extracted, out of which the graph kernel is computed, as a distance on probability distributions. The precise form of the pulse sequence is determined through training on a graph data set. Image from [Henry et al.](#)

## 14. COMPARISON BETWEEN THE DIFFERENT TARGETTED ARCHITECTURES

### DEVICE SPECIFICATIONS

To estimate the resources and requirements needed for the different hardware platforms that we are targeting to use for execution of our algorithms, we perform simulation estimations based on hardware devices. For each quantum computing architecture, we collect values for different system parameters based on recent experiments and we also provide some more optimistic hardware properties for the future. All future estimates are based on published roadmaps for different companies in the field and are optimistic estimates based on the development. The timelines on most roadmaps differ in terms of time and effort required, yet all anticipate a maximum outlook of a decade for future projections. The reason we perform future estimates for the time execution of different algorithms is to ensure that our results will be relevant and will be able to be used in parallel to the algorithmic development. The need of time for the scientific development throughout the project will require some time before all algorithmic components are ready to be executed and the parallel hardware development will lead to better and less error-prone (noisy) quantum processors (QPUs).

The hardware properties that we record and monitor are clock speed, 1-qubit gate fidelity, 2-qubit gate fidelity (both in digital and analog fashion), coherence time, reset/readout time, 1-qubit gate execution time and 2-qubit gate execution time.

The algorithmic parameters that define the simulation and the execution time of the experiments that are also of interest for us are the number of 1- and 2-qubit gates, the circuit execution and the algorithmic clock speed.

Specifications, values, and units recorded in our analysis are detailed in Table 1.

Table 1: Specification of Different Hardware Platforms (QPU and Algorithmic parameters) under consideration

<b>Neutral-atom qubits based QPUs</b>			
<i>Specifications</i>	<i>Unit</i>	<i>Current Estimates</i>	<i>Future Estimates</i>
# qubits	#	200	1000
Real clock speed	Hz	5 Hz	20 Hz
Algorithmic clock speed	Hz	5 Hz	20 Hz
Max # of parallel runs	#	10	10
1Q fidelity	%	NA	NA
2Q/analog fidelity	%	NA	NA
Coherence time (ms)	ms	30	30
Reset/readout (ms)	ms	200	50
1Q gates time (us)	µs	0.005	0.005
2Q gates time (us)	µs	0.5	0.5

<b>Superconducting qubits based QPUs</b>			
<i>Specifications</i>	<i>Unit</i>	<i>Current Estimates</i>	<i>Future Estimates</i>
# qubits	#	80	1000
Real clock speed	Hz	50 KHz	50 KHz
Algorithmic clock speed	Hz	50 KHz	4 KHz
Max # of parallel runs	#	1	1
1Q fidelity	%	99.7%	99.7%
2Q/analog fidelity	%	95%	99.98%
Coherence time (ms)	ms	0.0023	0.027
Reset/readout (ms)	ms	0	0
1Q gates time (us)	µs	0.006	0.006
2Q gates time (us)	µs	0.018	0.09

<b>Ion trap qubits based QPUs</b>			
<i>Specifications</i>	<i>Unit</i>	<i>Current Estimates</i>	<i>Future Estimates</i>
# qubits	#	11	1000
Real clock speed	Hz	8 KHz	8 KHz
Algorithmic clock speed	Hz	8 Hz	80 Hz
Max # of parallel runs	#	1	4
1Q fidelity	%	99.35%	99.9%
2Q/analog fidelity	%	99.6%	99.95%
Coherence time (ms)	ms	350	350
Reset/readout (ms)	ms	0.125	0.125
1Q gates time (us)	µs	10	10
2Q gates time (us)	µs	210	21

To ensure compatibility and to better understand the general QPU and Algorithmic specifications listed in Table 1, it is important to highlight the following remarks:

- The clock speed is measured differently for each device. For devices based on neutral atoms and trapped ions it is computed as  $1/(\text{reset and readout time})$  – since the reset and readout are the dominant process in terms of time consumption. For devices based on superconducting qubits, since the reset/readout time is negligible (active reset), the clock speed is computed as  $1/\text{coherence time}$ , which corresponds to the official specifications. This assumption is reasonable and is based on the different dominants time terms of each technology.
- The algorithmic clock speed is computed as the number of full algorithm circuit that the device can execute per second. For devices dominated by the gate time like ion trap qubit bases ones, this number can be very different from the actual clock speed. Also in the future estimates we estimated the increase of the circuit depth and number of gates in the parametrization in the estimation of the algorithmic clock speed.
- The maximum number of parallel runs is the maximum number of runs of the same (or very similar circuit) that can be executed at the same time on the device. This parameter is important when one considering the direction of parallel executions and multiple registers per experiment, although this is more of a far-term execution technique that would require significant development in the hardware platforms (mostly due to high noise effects).

## DEVICE SPECIFICATION ASSUMPTIONS

Herein we list all the assumptions we took into consideration when performing the estimations for different hardware architectures.

### Neutral Atom qubits based QPUs

For the case of neutral atom architecture, connectivity and qubit interaction map is vary a lot as a function of the distance and the influence of other qubits. A reasonable assumption for a successful and efficient experiment is an expected connectivity of **6** neighboring qubits, through a hexagonal lattice with a nearest-neighbor connectivity. In certain scenarios this connectivity map can be enriched with more-than-nearest neighbor connectivity, but the interaction terms may become prohibitive and limit the applicability of certain algorithmic schemes.

For the case of variational algorithms, we estimate the time for an entangling block to be in the order of 500 ns. For such architectures an entanglement block consists of a single analog block (qubit free or under a fixed Hamiltonian evolution) and the duration cannot be estimated from the number of restrictive multi-qubit operations, but only from the evolution time. The estimated number of layers to have a faithful execution of any of the algorithms we are targeting is set to 50. For the case of DQC and alike algorithms this number of entangling layers is sufficient to ensure efficient use of the high number of qubits provided, even for the NISQ era and the future expectations set for this qubit technology. For the case of variational algorithms, experiments found in the literature indicate that 50 layers are enough and will most probably be able to capture the properties of the systems under investigation at least for the

NISQ era. For the case of Quantum Evolution Kernel (QEK) 50 entanglement layers will create kernels that cannot be simulated classically and will be enough for the solution of the different targeted use for this particular algorithm.

Another important consideration of neutral-atom-based QPUs is the low clock speed that is a dominant factor for the circuit execution. A full circuit execution is fully dominated by the registry reset and readout time, since a circuit execution amounts in the order of  $10^{-2}$  ms, whereas reset and readout are in the order of 200-300 ms, leading to clock speeds in the order of 5Hz. At present, this constitutes the primary limiting factor. While there are several proposals and concepts under consideration, the implementation thereof is still ongoing. Although even after a one order of magnitude upgrade, the readout speed would still be the main limitation. We estimated a four-fold increase of the clock speed for the future hardware to render our assumption realistic.

### Superconducting qubits based QPUs

With the current specifications (coherence time, gate execution time, etc) of any superconducting qubit-based QPU, the execution of variational algorithms is limited to the toy problems that can be classically simulated. Any demonstrations in current literature have been proved to be classically simulated and thus most of our algorithmic schemes execution in large scale will be difficult to be done in superconducting qubit based architectures, mostly due to the high noise level, but also due to high gate overhead caused by the low connectivity.

Nevertheless, we perform our analysis based on assumptions both for current and for future estimates of the technology. First and foremost a significant limitation in superconducting qubit based QPUs is the limited connectivity between the qubits, that is predefined in the production of the QPU. For our analysis we estimate the connectivity of 3 neighboring qubits in the form of a honeycomb lattice. This connectivity is implementable, and we can reasonably assume that in the future such architectures will be created and used. Different limiting factors prohibit us from expecting higher connectivity for every qubit in the QPU, and even though in certain cases there may be qubits that will be interconnected more and in different lattice formations with their neighboring qubits, those cannot be the estimate of the norm.

We also assume that an entanglement block in a superconducting qubit based QPU will consist of order of 30 2-qubit gates. The estimate can vary a lot depending the number of qubits needed, but to make sure we are in a realistic scenario we choose to define an entanglement block that would be useful in the case of an 100 qubits experiment and consists of 18 SWAP operations and 12 CNOT gates. This is a conservative, but yet challenging approach for defining the Entanglement block on a Hardware efficient type of Ansatz. One should consider that with the current limited nominal capabilities we will be able to perform a maximum of 4 such entanglement blocks in order to acquire meaningful results considering current QPU specifications and executions times. State-of-the-art literature clearly indicates that 4 entanglement layers (or 4 layers of hardware efficient Ansatz blocks) will not be enough and the number is way too low to acquire a trial wavefunction with the expressivity and entanglement strength needs. For the case of DQC the requirements for representing different dimensions for solving differential equations successfully will not be fulfilled and the same argument will hold for the case of variational algorithms. Another important remark is that 4 entangling layers in a 100 qubit register remains a problem that can be classically simulated using tensor networks and still does not outperform current CPU capabilities, meaning that our experiments will not be out of reach for current computers. Possibly increasing the number of entanglement blocks to 50-100 will lead to circuits that are of high interest but this would also require increase in the coherence time in the order of 10 times and 1000 times better

fidelities in 2-qubit gate operations. These estimates are still to be achieved and to the best of our estimates will not be reached within the duration of the project and when we would like to perform our experiments, thus we follow a more conservative approach for our future QPU specifications.

### Trapped ion qubits based QPUs

Considering ion trap-based quantum processors, the connectivity for these devices is not an issue at hand. The intrinsic properties of the system allow for an all-to-all connectivity reducing the overhead of swapping qubits that can significantly increase the circuit depth. This particular device specification increases the near-term applicability and allows for better implementation with less limitations for our algorithmic schemes.

For the case of ion trap qubit-based platforms, an entangling layer for a 100-qubit register comparable to the one we used for superconducting qubit based platforms would require the use of 12 entangling gates (CNOTs). Considering the 2-qubit gate execution time and the available coherence time we can estimate that with the current setups one would be able to perform calculations using an order of 50 entangling layers. Experiments found in the literature do not demonstrate such high circuit depth (around 600 gates), but it is theoretically possible for the specifications the hardware of today has. This is mostly attributed to the fact that ion-trap qubits have high coherence times and although the gate execution time is a dominant factor the number of gates that can be effectively performed remains large. The total execution time for a circuit in these particular devices amounts for milliseconds (which is orders of magnitude higher than to the other platforms in this comparison) and is the limiting factor for the circuit repetition rate, essential for the variational schemes. Readout and reset process are in the order of  $10^{-2}$  ms, whereas a single 2-qubit gate execution amounts to the order of  $10^2$  ms. The potential for addressing this issue is high and future device are estimated to increase at least (10 times and more) the performance in terms of circuit execution time.

Another important aspect is the gate fidelity estimated. For our characterization purposes we estimated a fidelity of 0.999 (or 99.9%) which is higher than the usual recorded values (99.7-99.8%). The reason for this estimate mainly lies in the fact that 99.9% fidelity is already recorded and there is a high probability that with the hardware will evolve rapidly in this direction, benefiting our implementation. Practically, this means that the device will be able to execute a 50-layer entanglement block (600 gates) with a circuit fidelity above 50% (computed as  $0.999^{600}=0.549$  or 54.9%), potentially leading to meaningful results.

## ALGORITHM SPECIFICATION ASSUMPTIONS

### Differentiable Quantum Circuits (DQC) Algorithm

For the case of DQC-based algorithms we want to solve a partial differential equation. In order to perform such a calculation in a system of 100 qubits (which is a reasonable estimate for a quantum advantage type of demonstration) we will need 200 circuits for the differentiation. If we consider a 1<sup>st</sup> order differential equation in a 2D or 3D domain, also including the time dimension, we will need roughly half the number of qubits in entanglement layers, meaning 50 entanglement layers. For the case of superconducting qubit based QPUs in the currently available setups we set this value to 3, since this is what can realistically be done, but in our future estimates we perform the same analysis for the required 50 layers. On the training domain we also set the number of points to be 100.

For each circuit we would like to perform at least a small number of repetitions (5 shots). This number may seem quite low, but in our algorithmic development (Equality project WP1) we noticed that we can still acquire good solutions within a small range of shots for a fixed budget. One can see the number of shots also a pre-factor that does not change the relative behavior or the comparison in between different platform architectures. We also consider a single epoch per problem instance, since we are targeting the kernel DQC approach, but even if the epochs increase via a classical feedback loop again this should only be a pre-factor that does not change the comparison between platforms.

### Variational Algorithms

Variational Algorithms are also quite demanding in terms of resources and in the last years have been used extensively to benchmark different hardware platforms. In our case we base our estimates on a circuit comprising from 50 layers and we try to solve an optimization problem. The reason we choose this problem is to mitigate the effect of the number of operators to be measured. In cases like chemistry or high energy physics the number of operators to be measured grows quite fast and each operator (or set of operators) requires a postprocessing on the circuit to ensure the right computational basis. For this reason, we target a Minimum Independent Set (MIS) problem without loss of generality.

For the classical feedback loop, we consider 100 optimization steps (epochs) which should be enough for a well-defined problem, but it is also highly dependent on the optimization algorithm being used.

### Quantum Evolution Kernel Algorithm

For graph machine learning algorithms, like the Quantum Evolution Kernel method, we believe that in the range of 100 qubits we will be able to demonstrate interesting simulations and solve problems of relevant interest. The number of entanglement layers that will be needed is again in the order of 50 layers, to ensure enough expressivity for our circuit.

For QEK, the number of shots per circuit execution should be slightly higher than for DQC based experiments and from our algorithmic development effort we have estimated that we need at least 100 repetitions (shots) per circuit and for the classical feedback loop we estimate roughly 1000 epochs to acquire meaningful results.

## RESULTS

### Algorithm Execution Times

An important parameter that will define the feasibility of the approach is the time that an algorithm would require to be executed in the quantum hardware. Based on the assumption we enumerated in the previous sections we perform estimates and report the execution time for different algorithmic instances and different hardware specifications. In Figure 5 we give a histogram for the execution times of different algorithms in different devices.

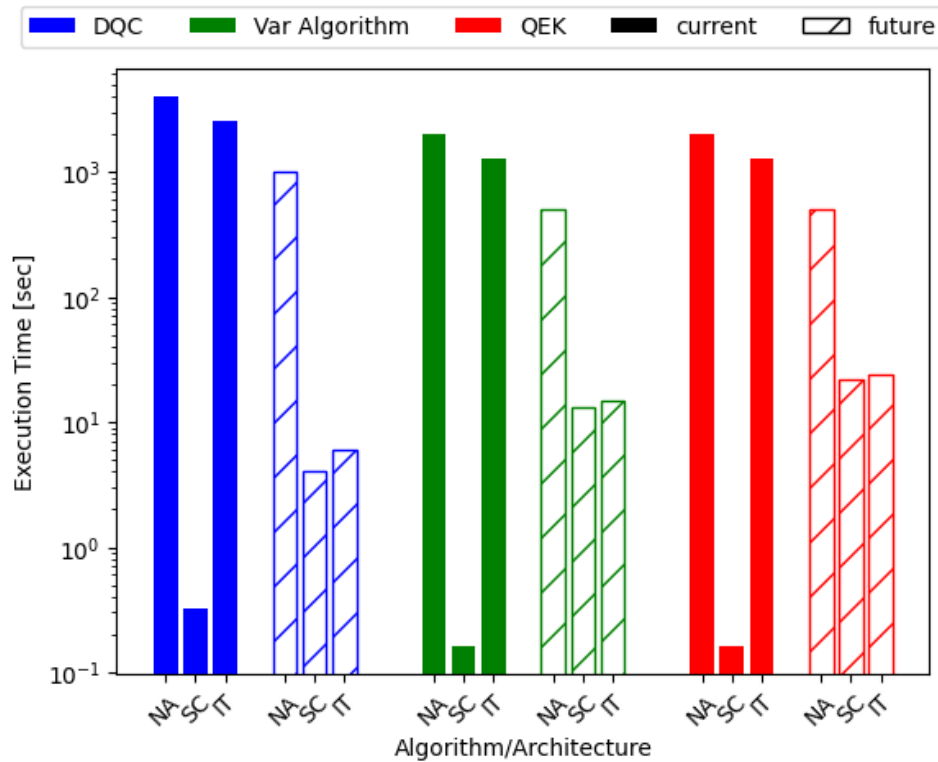


Figure 5: Execution times for the different hardware platforms and algorithms under consideration. Different colors denote different algorithms and different bar fillings denote current (solid bars) and future (striped bars) architectures. For each algorithm we record the execution time for Neutral Atom (NA), Superconducting (SC) and Ion Trap (IT) based devices.

It is clear that superconducting qubits are the ones having the minimum requirements in terms of execution time which is mostly attributed to the fact that the 2-qubit gates can be performed much faster, but the coherence time of these devices is also significantly less comparing to the rest of the architectures. One should take into consideration also these parameters when trying to compare different architectures and an important aspect to highlight is the ratio between circuit execution time and coherence time of the device in the near- and longer-term estimates (shown in Figure 6).



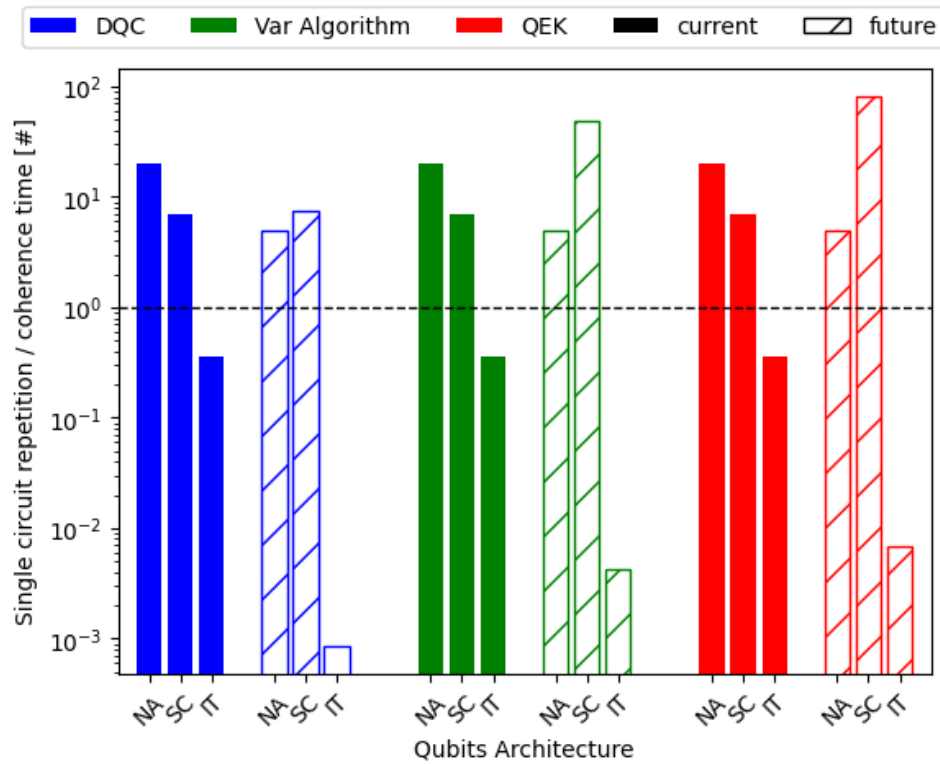


Figure 6: Ratio between the single circuit execution (shot) over the available decoherence time of the specific qubit architecture. Different colors denote different algorithms and different bar fillings denote current (solid bars) and future (striped bars) architectures. For each algorithm we record the relevant ratio for Neutral Atom (NA), Superconducting (SC) and Ion Trap (IT) based devices.

In Table 2 we record all the data we used for our algorithmic experiments and the relevant data we used to compare algorithmic schemes in different QPU architectures.

Table 2: Comparison of execution times for all three algorithms and all three hardware platforms, simulations (as *current*) and prediction (as *future*). We record all the circuit specific information that we used to estimate the time.

<b>Differentiable Quantum Circuits Algorithm</b>					
<i>Platform</i>	<i># gates/layer</i>	<i># layers</i>	<i># gates</i>	<i># shots</i>	<i>Execution time (sec)</i>
Neutral Atom (current)	1	50	50	20000	4000
Neutral Atom (future)	1	50	50	20000	1000
Superconducting (current)	30	3	90	20000	0.324
Superconducting (future)	30	50	1500	20000	5.4
Ion Trap (current)	12	50	600	20000	2522.5
Ion Trap (future)	12	50	600	20000	254.5

<b>Variational Algorithm</b>					
<i>Platform</i>	<i># gates/layer</i>	<i># layers</i>	<i># gates</i>	<i># shots</i>	<i>Execution time (sec)</i>
Neutral Atom (current)	1	50	50	10000	2000
Neutral Atom (future)	1	50	50	10000	500
Superconducting (current)	30	3	90	10000	0.162
Superconducting (future)	30	50	1500	10000	2.7
Ion Trap (current)	12	50	600	10000	1261.25
Ion Trap (future)	12	50	600	10000	127.25

<b>Quantum Evolution Kernel Algorithm</b>					
<i>Platform</i>	<i># gates/layer</i>	<i># layers</i>	<i># gates</i>	<i># shots</i>	<i>Execution time (sec)</i>
Neutral Atom (current)	1	50	50	10000	2000
Neutral Atom (future)	1	50	50	10000	500
Superconducting (current)	30	3	90	10000	0.162
Superconducting (future)	30	50	1500	10000	2.7
Ion Trap (current)	12	50	600	10000	1261.25
Ion Trap (future)	12	50	600	10000	127.25

### Algorithms Feasibility

To better understand the effect of the hardware specifications we try to estimate when the algorithms that we are developing will become relevant for demonstrating interesting and classically intractable problems. In Figure 7 and Figure 8 we try to estimate this region in terms of 2-qubit gates fidelity and coherence time for the different QPU architectures. For the case of neutral-atom-qubit based architectures we do not perform the same analysis since it will be difficult to perform such estimates for analog or analog-digital setups.

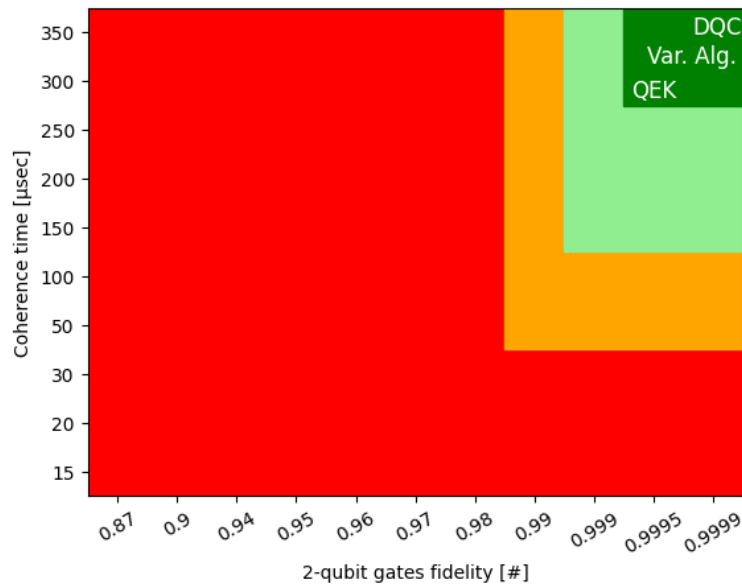


Figure 7: Feasibility of Algorithms in Superconducting-qubit-based platforms in dependence of 2-qubit gate fidelity and coherence time

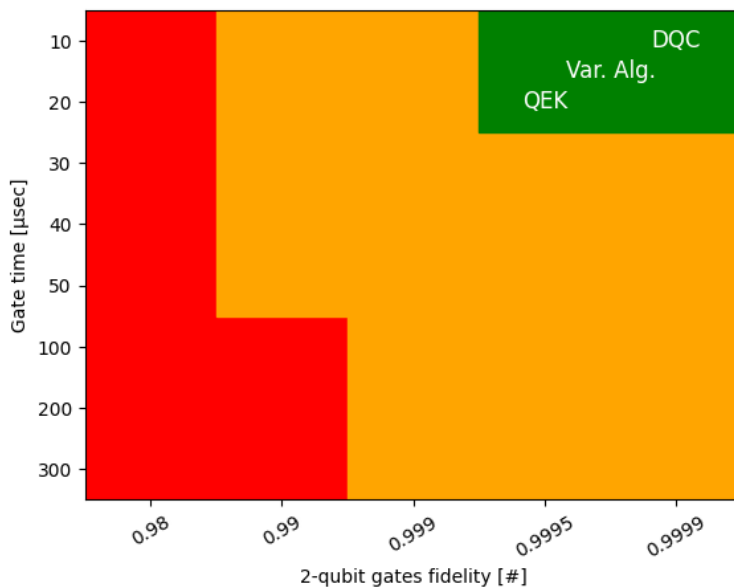


Figure 8: Feasibility of Algorithms in Ion-Trap-qubit-based platforms in dependence of 2-qubit gate fidelities and gate time.

From Figure 7 and Figure 8 above it becomes clear and evident that the current hardware specifications can be a limiting factor for our algorithmic implementations, but it is also evident that with the hardware evolution and the advancement of the technology we will be able to perform relevant simulations that will have significant impact. This synergetic development would also benefit from the algorithmic development, since many of the estimated requirements will be decreased and the potential to implement the algorithms in a more efficient way will be materialized.

## 15. CONCLUSIONS

In conclusion, the analysis of different qubit architectures and quantum algorithms has revealed several key insights and considerations regarding the feasibility of quantum computing. While quantum computing holds immense promise for revolutionizing various fields, there are inherent challenges and limitations that must be addressed as the technology continues to evolve.

Our examination of various architectures, including neutral-atom-based, superconducting-based and trapped-ion-based qubits, highlights the diversity in approaches. Each architecture has its unique advantages and disadvantages. Selecting the most appropriate qubit architecture depends on the specific application and the corresponding requirements.

We studied various near term quantum algorithms in order to demonstrate their potential to solve certain problems that are of interest for our project. We chose these algorithms specifically for the use cases we are targeting and also considering the fact that we will be able to optimise the resources and the calculation overhead throughout the rest of the project. With our analysis it becomes clear that the algorithmic development needs to happen in parallel with the hardware architecture evolutions and presents an ongoing challenge. Further research is necessary to expand the algorithm capabilities and reduce the required resources to make them more feasible in current and near-future hardware.

It is important to highlight the fact that despite the existing limitations, quantum computing continues to advance rapidly. Research and development efforts, including the one presented herein, are focused on hardware scalability and discovery of new quantum algorithms. As these areas progress, we anticipate that the feasibility and practicality of quantum computing will continue to improve.

## 16. BIBLIOGRAPHY

- [Adams2020] C. S. Adams et al., J. Phys. B: At. Mol. Opt. Phys. 53, 012002 (2020)
- [Ashkin2018] <https://www.nobelprize.org/prizes/physics/2018/summary/>
- [Ballance2015] C. J. Ballance et al., Nature 528, 384–386 (2015)
- [Bermudez2017] A. Bermudez et al., Phys. Rev. X 7, 041061 (2017)
- [Bremner2002] M. J. Bremner et al., Phys. Rev. Lett. 89, 247902 (2002)
- [Bruzewicz2019] C. D. Bruzewicz et al., Appl. Phys. Rev. 6, 021314 (2019)
- [Browaeys2020] A. Browaeys and T. Lahaye, Nat. Phys. 16, 132–142 (2020)
- [Brylinski2002] R. K. Brylinski and G. Chen, Mathematics of quantum computation, CRC Press, (2002)
- [Cirac1995] J. I. Cirac and P. Zoller, Phys. Rev. Lett. 74, 4091 (1995)
- [Ding2023] L. Ding et al., Phys. Rev. X 13, 031035 (2023)
- [Dodd2002] J. L. Dodd et al., Phys. Rev. A 65, 040301 (2002)
- [FSKYT] [Mechanical Paul trap](#)
- [Harty2014] T. P. Harty et al., Phys. Rev. Lett. 113, 220501 (2014)
- [Henriet2020] L. Henriet et al., Quantum 4, 327 (2020)
- [Hempel2018] C. Hempel et al., Phys. Rev. X 8, 031022 (2018)
- [Henry2021] L. P. Henry et al., Phys. Rev. A 104, 032416 (2021)
- [Isenhower2010] L. Isenhower et al., Phys. Rev. Lett. 104, 010503 (2010)
- [IonTrappingWW] <https://quantumoptics.at/en/links/ion-trapping-worldwide.html>
- [IQMVT] <https://thequantuminsider.com/2023/10/10/finland-launches-a-20-qubit-quantum-computer/>
- [Jaksch2000] D. Jaksch et al., Phys. Rev. Lett. 85, 2208 (2000)
- [Kandala2017] A. Kandala et al., Nature, 549, 242–246 (2017)
- [Kandala2018] A. Kandala et al., Nature volume 567, pages 491–495 (2019)
- [Kleine2011] G. Kleine Büning et al., Phys. Rev. Lett. 106, 240801 (2011)

- [Kyriienko2021] O. Kyriienko, A. E. Paine, and V. E. Elfving, Phys. Rev. A 103, 052416 (2021)
- [Levine2018] H. Levine et al., Phys. Rev. Lett., 121, 123603 (2018)
- [Levine2019] H. Levine et al., Phys. Rev. Lett. 123, 170503 (2019)
- [Madjarov2020] I. S. Madjarov et al., Nat. Phys. 16, 857–861 (2020)
- [McClellan2016] J. R. McClellan et al., New J. Phys. 18 023023 (2016)
- [Michel2023] A. Michel et al., Phys. Rev. A 107, 042602 (2023)
- [Nogrette2014] F. Nogrette et al., Phys. Rev. X 4, 021034 (2014)
- [O'Malley2016] P. J. J. O'Malley et al., Phys. Rev. X 6, 031007 (2016)
- [ParraRodriguez2020] A. Parra-Rodriguez et al., Physical Review A 101, 022305 (2020)
- [Peruzzo2014] A. Peruzzo et al., Nature Communications volume 5, 4213 (2014)
- [Pogorelov2021] I. Pogorelov et al., PRX Quantum 2, 020343
- [QuantinumVolume] <https://www.quantinum.com/news/quantum-volume-reaches-5-digits-for-the-first-time-5-perspectives-on-what-it-means-for-quantum-computing>
- [QuantinumQCCD] <https://www.forbes.com/sites/moorinsights/2023/04/03/unlocking-quantum-potential-with-high-quality-qubits-how-quantinum-achieved-a-three-year-string-of-record-breaking-quantum-measurements/>
- [Ruster2016] T. Ruster et al., Appl. Phys. B 122, 254 (2016)
- [Saffman2010] M. Saffman et al., Rev. Mod. Phys. 82, 2313 (2010)
- [Schäfer2018] V. M. Schäfer et al., Nature 555, 75–78 (2018)
- [Schreck2021] F. Schreck et al., Nature Physics 17, 1296–1304 (2021)
- [Shen2017] Y. Shen et al., Phys. Rev. A 95, 020501 (2017)
- [Sørensen1999] A. Sørensen and K. Mølmer, Phys. Rev. Lett. 82, 1971 (1999)
- [Tilly2022] J. Tilly et al., Physics Reports, 986 (2022)
- [UnivQuantum] <https://universalquantum.com>
- [Wurtz2023] Aquila: QuEra's 256-qubit neutral-atom quantum computer
- [Zervas2014] M. N. Zervas and C. A. Codemard, IEEE Journal of Selected Topics in Quantum Electronics, 20, 5, 219-241 (2014)